Iron Halide Mediated Atom Transfer Radical Polymerization of Methyl Methacrylate with *N*-Alkyl-2-pyridylmethanimine as the Ligand

HUIQI ZHANG, ULRICH S. SCHUBERT

Laboratory of Macromolecular Chemistry and Nanoscience, Eindhoven University of Technology and Dutch Polymer Institute, P. O. Box 513, 5600 MB Eindhoven, The Netherlands

Received 19 February 2004; accepted 4 May 2004
DOI: 10.1002/pola.20289
Published online in Wiley InterScience (www.interscience.wiley.com).

ABSTRACT: The controlled atom transfer radical polymerization (ATRP) of methyl methacrylate (MMA) catalyzed by iron halide/*N*-(*n*-hexyl)-2-pyridylmethanimine (NHPMI) is described. The ethyl 2-bromoisobutyrate (EBIB)-initiated ATRP with $[MMA]_0/[EBIB]_0/[\text{iron halide}]_0/[NHPMI]_0 = 150/1/1/2$ was better controlled in 2-butanone than in *p*-xylene at 90 °C. Initially added iron(III) halide improved the controllability of the reactions in terms of molecular weight control. The *p*-toluenesulfonyl chloride (TsC1)-initiated ATRP were uncontrolled with $[MMA]_0/[TsC1]_0/[\text{iron halide}]_0/[NHPMI]_0 = 150/1/1/2$ in 2-butanone at 90 °C. In contrast to the EBIB-initiated system, the initially added iron(III) halide greatly decreased the controllability of the TsC1-initiated ATRP. The ration of iron halide to NHPMI significantly influenced the controllability of both EBIB and TsC1-initiated ATRP systems. The ATRP with $[MMA]_0/[\text{initiator}]_0/[\text{iron halide}]_0/[NHPMI]_0 = 150/1//1/2$ provided polymers with PDIs ≥ 1.57, whereas those with $[\text{iron halide}]_0/[NHPMI]_0 = 1$ resulted in polymers with PDIs as low as 1.35. Moreover, polymers with PDIs of approximately 1.25 were obtained after their precipitation from acidified methanol. The high functionality of the halide end group in the obtained polymer was confirmed by both ^1H NMR and a chain-extenstion reaction. Cyclic voltammetry was utilized to explain the differing catalytic behaviors of the *in situ*-formed complexes by iron halide and NHPMI with different molar ratios. © 2004 Wiley Periodicals, Inc. J Polym Sci Part A: Polym Chem 42: 4882–4894, 2004

Keywords: atom transfer radical polymerization (ATRP); catalysts; deactivator; iron halide; living polymerization; methyl methacrylate; *N*-(*n*-hexyl)-2-pyridylmethanimine

INTRODUCTION

Controlled/living radical polymerization techniques have revolutionized the field of free-radical polymerization in the past decade, which provides polymers with predetermined molecular weights, low polydispersities, specific functionalities, and various architectures under relatively mild reaction conditions.[1–3] Atom transfer radical polymerization (ATRP) is one of the most versatile systems, because of the easy availability of many kinds of initiators, catalysts, and monomers.[4,5] There exists a reversible dynamic equilibrium between the dormant species (alkyl halide or arenesulfonyl halide) and active species (radicals) in ATRP, which controls the radical concentrations and, thus, the controllability of the

Correspondence to: U. S. Schubert (E-mail: u.s.schubert@tue.nl)

Journal of Polymer Science: Part A: Polymer Chemistry, Vol. 42, 4882–4894 (2004)

ATRP systems. The catalysts (metal salts/ligands) have a significant influence on equilibrium and thus play an important role in ATRP. Thus far, a number of different metal–ligand combinations have been investigated, including systems based on Cu,[6–12] Ru,[13–17] Pd,[18] Rh,[19] Ni,[20–23] Re,[24] Mo,[25,26] Co,[27] and Fe.[28–42] Of these, iron offers particular attraction because of its low cost, low toxicity, and biocompatibility.

Recently, iron-based catalysts containing imine ligands have drawn a great deal of attention in ATRP.[35,39–42] Gibson et al. reported a series of highly active iron halide-based catalysts bearing tridentate salicylaldiminato ligands for the ATRP of styrene, wherein reactions proceeded quite quickly and provided polymers with very low polydispersity indices (PDIs, typically ca. 1.10).[41] They also used $FeCl_2$ complexes bearing α-diimine ligands for the polymerization of methyl methacrylate (MMA)[40] and styrene.[39] The α-diimine ligands containing alkylimino substituents induced well-controlled ATRP of both MMA and styrene, whereas those with arylimino substituents gave rise to chain-transfer processes.[39,40] *N*-Alkyl-2-pyridylmethanimines and their derivatives were also utilized in the iron-mediated ATRP systems.[35,42] Matyjaszewski et al. described the use of a diiminopyridine–$FeBr_2$ complex for the ATRP of MMA, but the reaction was not controlled.[35] Gibson et al. applied a series of preformed complexes of $FeCl_2$ with *N*-alkyl-2-pyridylmethanimines (and their derivatives) in the ATRP of both MMA and styrene.[42] The ATRP of styrene was controlled, whereas the results from the ATRP of MMA were not satisfactory. The polymerization of MMA with 2-(*N*-cyclododecylimino)-6-methylpyridine as the ligand provided optimal results, but the PDIs of the resulting polymers were still rather high (PDIs = 1.49–1.64, depending on the initiators used), even after the precipitation of polymers from acidified methanol solutions (5% HCl, v/v). It is known that low-molecular-weight PMMA may be soluble in methanol and thus purification of the obtained polymers by precipitating into methanol results in lower PDIs (see ref. 36 and Table 1 in this article). Further, the reactions were rather slow (32 h for a full conversion). Therefore, the utilization of *N*-alkyl-2-pyridylmethanimines and their derivatives in the iron-mediated ATRP of MMA has achieved little success, although they are very effective ligands for the copper-mediated ATRP of MMA,[43–47] styrene,[48,49] and butyl acrylate.[50]

Very recently, we reported an efficient iron(II) bromide-based catalyst bearing *N*-(*n*-hexyl)-2-pyridylmethanimine (NHPMI) ligand for the ATRP of MMA, where fast polymerizations, linear progress of molecular weights with monomer conversions, and low polydispersities of the polymers were achieved.[51] Compared with the ligand 2-(*N*-cyclododecylimino)-6-methylpyridine,[42] NHPMI can be prepared at a much lower cost, which makes it a very attractive ligand for potential practical application. In this article, we describe our systematic studies on the iron halide mediated ATRP of MMA with NHPMI as the ligand. The effects of the utilized solvents, initially added iron(III) halide, reaction temperature, molar ratio of iron halide to NHPMI, initiators, and the catalyst (iron halide/NHPMI) concentrations on the polymerizations are reported in detail. In particular, the significant effect of molar ratio of iron halide to NHPMI on the controllability of the studied ATRP systems is highlighted. Cyclic voltammetry analysis was performed for the *in situ*-formed complexes by iron(II) halide and NHPMI with different molar ratios, in order to gain a better understanding of the underlying phenomena. Furthermore, the high functionality of the halide end group in a polymer prepared via ATRP was also verified with the ^1H NMR technique and a chain-extension reaction.

EXPERIMENTAL

Materials

MMA (Aldrich; 99%) was washed twice with an aqueous solution of sodium hydroxide (5%) and twice with distilled water, dried with anhydrous magnesium sulfate overnight, and then distilled over calcium hydride *in vacuo*. The distillate was stored at −25 °C before use. 2-Butanone (Acros; >99%) was used as received in the ethyl 2-bromoisobutyrate (EBIB)-initiated ATRP; it was dried with calcium hydride overnight and then distilled before its use in the *p*-toluenesulfonyl chloride (TsCl)-initiated ATRP. NHPMI was synthesized by condensation of pyridine-2-carboxaldehyde (Acros; 99%) and *n*-hexylamine (Acros; 99%), as described elsewhere.[43] $FeBr_2$ (Aldrich; 98%), $FeCl_2$ (Aldrich; anhydrous, beads, −10 mesh, 99.99%), $FeBr_3$ (Aldrich; 98%), $FeCl_3$ (Acros; anhydrous, 98%), EBIB (Aldrich; 98%), TsCl (Acros; 99%), *p*-xylene (Aldrich; 99%; anhydrous), deuterated methylene chloride (CD_2Cl_2, Cam-

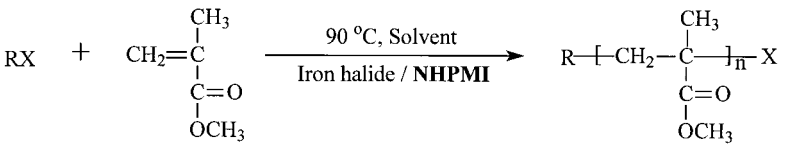

Scheme 1. Schematic presentation of the ATRP of MMA.

bridge Isotope Laboratories, Inc.; 99.9%), aluminum oxide (Acros; activated, neutral, for column chromatography 50–200 μm), and all other chemicals were used as received.

General Procedure for the ATRP of MMA

$FeBr_2$ (0.2052 g, 0.951 mmol), $FeCl_3$ (0.0324 g, 0.200 mmol), and NHPMI (0.2209 g, 1.161 mmol) were added to a mixture of MMA (14.2308 g, 142.137 mmol) and 2-butanone (24.2481 g) in a three-necked round-bottom flask (100 mL). The reaction mixture was bubbled with argon for 40 min at room temperature, and the flask was then immersed in a thermostated oil bath at 90 °C and stirred for 1 h. The initiator EBIB (0.1905 g, 0.977 mmol) was added slowly (over 2 min) into the system to start the reaction. The polymerization was sampled at suitable time periods throughout the reaction. The samples were diluted with tetrahydrofuran (THF), and parts of them were used for gas chromatography (GC) measurements to determine monomer conversions. Other parts of the remaining samples were passed through activated neutral aluminum oxide columns before size exclusion chromatography (SEC) measurements. To compare with the literature results,[42] some samples were also purified by precipitation from 20-fold volume excess of rapidly stirred acidified methanol solutions (5% HCl, v/v) before SEC measurements.

Measurements

Monomer conversions were determined from the concentrations of the residual monomer with an Interscience Trace GC with an auto-sampler, equipped with an Rtx-5 (Crossbond 5% diphenyl–95% dimethyl polysiloxane) capillary column with the reaction solvent (*p*-xylene and 2-butanone) as the internal reference. Molecular weights and PDIs of the polymers were measured with a Waters SEC equipped with a Waters model 510 pump and a model 410 differential refractometer (40 °C). THF was used as the eluent at a flow rate of 1.0 mL/min. A set of two linear columns (Mixed-C, Polymer Laboratories, 30 cm, 40 °C) was used. The calibration curve was prepared according to polystyrene (PS) standards, and molecular weights were recalculated with the universal calibration principle and Mark–Houwink parameters (PS: $K = 1.14 \times 10^{-4}$ dL g^{-1}, $\alpha = 0.716$; PMMA: $K = 0.944 \times 10^{-4}$ dL g^{-1}, $\alpha = 0.719$). ^{1}H NMR spectrum of the polymer was recorded on a Varian 400 MHz spectrometer with CD_2Cl_2 as the solvent. Cyclic voltammetry (CV) analysis was performed at room temperature in a nitrogen atmosphere, using an Ecochemie Autolab PGSTAT30 potentiostat, which used an Ag counter electrode, Pt working electrode, and a Ag/AgCl reference electrode with [^{n}Bu$_4$N][PF$_6$] (0.1 M) as an electrolyte (sweep rate: 200 mV). The ferrocene(II)/(III) couple ($E_{1/2}$ = 450 mV and ΔE_p = 280 mV) was utilized as a benchmarked redox couple. The solutions of FeX_2 (X = Br and Cl) and NHPMI in dry 2-butanone were bubbled with argon for 40 min and then magnetically stirred at 90 °C for 1 h under argon. The obtained complex solutions were used for the CV measurements.

RESULTS AND DISCUSSION

Iron Halide Mediated ATRP of MMA with EBIB as the Initiator

Effect of Solvents on Polymerization

The ATRP of MMA with EBIB as the initiator and $FeBr_2$/NHPMI as the catalyst was carried out at 90 °C in 2-butanone and *p*-xylene, respectively, to study the effect of the utilized solvents on polymerization (Scheme 1). The volume of the solvent used was twice that of MMA in each ATRP system, and the molar ratio of MMA to EBIB to $FeBr_2$ to NHPMI was 150:1:1:2. The ATRP of

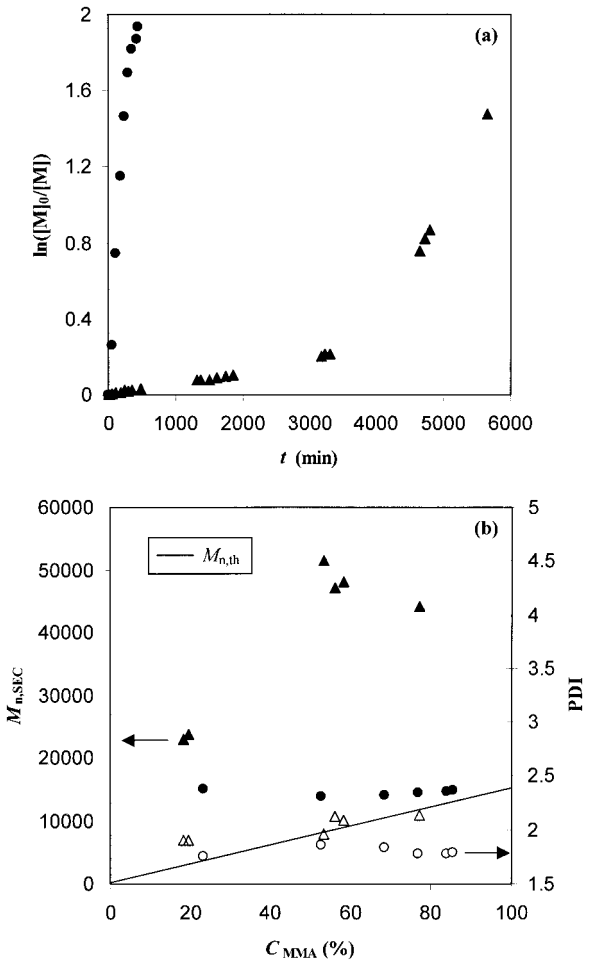

Figure 1. (a) Kinetic plots of $\ln([M]_0/[M])$ versus reaction time t and (b) dependence of $M_{n,SEC}$ (filled symbols) and PDIs (empty symbols) of the polymers on C_{MMA} for the ATRP of MMA at 90 °C with 2-butanone (●) and *p*-xylene (▲) as the solvent, respectively. $[MMA]_0/[EBIB]_0/[FeBr_2]_0/[NHPMI]_0$ = 150/1/1/2, MMA/solvent = 1/2 v/v.

MMA in *p*-xylene was heterogeneous, with a dark purple optical appearance, whereas that in 2-butanone was homogeneous, with a dark brown color, when the reaction temperature was 90 °C.

Figure 1(a) shows the kinetic plots of polymerizations in different solvents. The polymerization proceeded much faster in 2-butanone than in *p*-xylene, probably because of the different homogeneity of the reaction systems in different solvents. The monomer conversion (C_{MMA}) reached 86% at a reaction time (t) of 540 min in 2-butanone and 77% at t = 5640 min in *p*-xylene, respectively. The polymerization rate in 2-butanone was rather fast throughout the reaction and slightly decreased during the reaction process, whereas that in *p*-xylene was very slow in the first 3300 min and then dramatically increased. The molecular weights of the polymers determined by SEC (i.e., $M_{n,SEC}$) were much closer to the theoretical molecular weights (i.e., $M_{n,th} = ([M]_0/[RX]_0)M_M C_M + M_{RX}$, where $[M]_0$ and $[RX]_0$ are the initial concentrations of monomer and initiator, respectively, M_M and M_{RX} are the molecular weights of monomer and initiator, respectively, and C_M is the monomer conversion) in 2-butanone than in *p*-xylene, and the PDIs of the polymers obtained in 2-butanone were also much lower than those obtained in *p*-xylene [Fig. 1(b)]. All these results indicated that 2-butanone was a better solvent than *p*-xylene for the studied polymerization. Therefore, 2-butanone was used as the solvent in the following studies.

Effect of Initially Added Iron(III) Halide on the Polymerization Process

The addition of a certain amount of deactivator (metal salt in its higher oxidation state) at the beginning of the reaction has proven to be helpful in improving the controllability of the ATRP system.[33,46,47] Therefore, iron(III) halide was added to the ATRP system with $[MMA]_0/[EBIB]_0/[FeBr_2]_0/[NHPMI]_0$ = 150/1/1/2 at the beginning of the reaction to study its effect on the polymerization process. The initially added iron(III) halide indeed improved the molecular weight control of the system; that is, $M_{n,SEC}$ started to increase with C_{MMA} throughout the reaction and the PDIs of the polymers decreased largely with the addition of iron(III) halide [Figs. 2(b) and 3(b)]. The amounts of the initially added iron(III) halide had little influence on the kinetics of the reactions, molecular weights, or PDIs of the polymers (Figs. 2, 3). However, the type of iron(III) halide used did have some influence on the polymerization behavior. The addition of $FeBr_3$ into the reaction system appeared to result in the loss of the halide end group of the polymers after 300 min, as demonstrated by the leveling-off of the kinetic plots of the reactions after 300 min [Fig. 2(a)]. This phenomenon was not observed in either the ATRP system without initially added iron(III) halide or that with initially added $FeCl_3$ [Fig. 3(a)]. Further investigation is ongoing to provide a reasonable explanation.

The $FeCl_2$-mediated ATRP of MMA was also carried out in 2-butanone at 90 °C with $[MMA]_0/[EBIB]_0/[FeCl_2]_0/[NHPMI]_0$ = 150/1/1/2 and a volume ratio of MMA to 2-butanone of 1/2 [Fig. 4(a,b)].

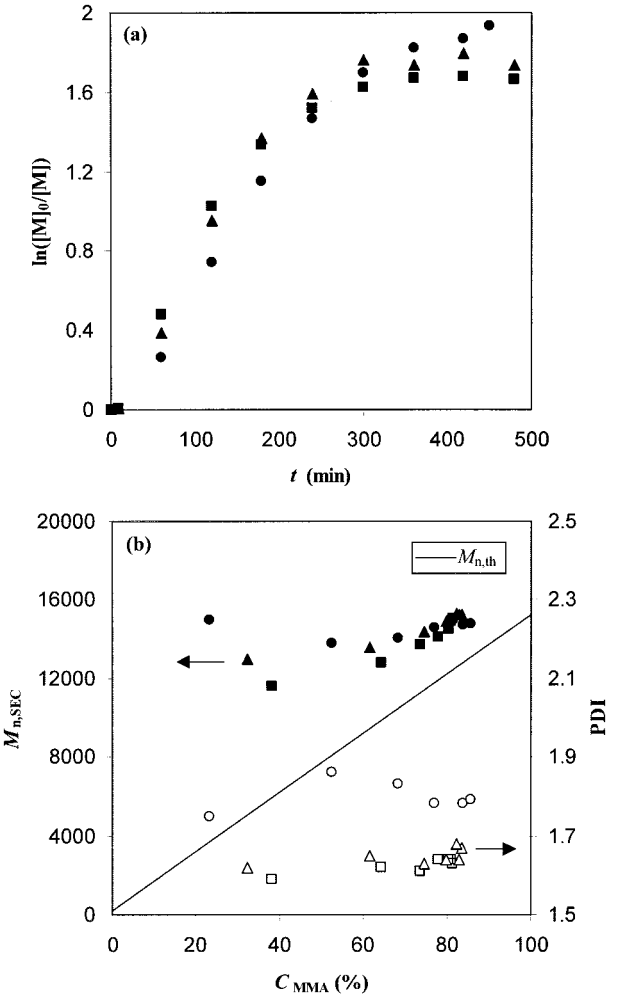

Figure 2. (a) Kinetic plots of $\ln([M]_0/[M])$ versus reaction time t and (b) dependence of $M_{n,SEC}$ (filled symbols) and PDIs (empty symbols) of the polymers on C_{MMA} for the $FeBr_2$-mediated ATRP of MMA with different amounts of initially added $FeBr_3$. $[MMA]_0/[EBIB]_0/[FeBr_2]_0/[FeBr_3]_0/[NHPMI]_0$ = 150/1/1/0/2 (●), 150/1/1/0.2/2.4 (▲), and 150/1/1/0.7/3.4 (■), MMA/2-butanone= 1/2 v/v, reaction temperature: 90 °C.

The curved kinetic plot of $\ln([M]_0/[M])$ versus t (symbol ●) suggested the existence of radical termination during the reaction. The $M_{n,SEC}$ first decreased and then increased with C_{MMA}. The PDIs of the obtained polymers decreased with C_{MMA}, but were still very high at high C_{MMA} (PDI = 1.95 at a C_{MMA} = 80%). The controllability of the polymerization was also improved with the addition of $FeCl_3$ at the beginning of the reaction. The kinetic plot of $\ln([M]_0/[M])$ versus t gradually changed from a curved to a linear form when the amount of initially added $FeCl_3$ increased from 20% to 60% relative to $FeCl_2$. The $M_{n,SEC}$ of the polymers started to increase linearly with C_{MMA}, and the PDIs of the polymers decreased greatly, down to 1.57 at a C_{MMA} = 80%. However, the amount of the initially added $FeCl_3$ had little influence on the $M_{n,SEC}$ and PDIs of the obtained polymers.

Effect of Reaction Temperature on Polymerization

The $FeCl_2$-mediated ATRP of MMA with $[MMA]_0/[EBIB]_0/[FeCl_2]_0/[FeCl_3]_0/[NHPMI]_0$ = 150/1/1/0.2/2.4 was carried out in 2-butanone (MMA/2-butanone = 1/2 v/v) at 90 and 75 °C, respectively, to study the influence of reaction temperature on

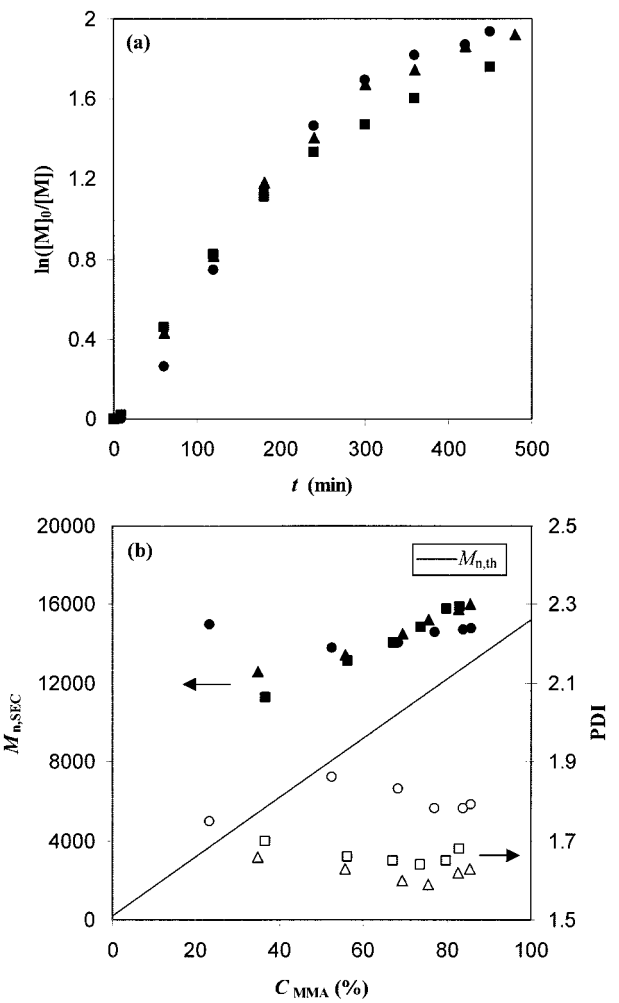

Figure 3. (a) Kinetic plots of $\ln([M]_0/[M])$ versus reaction time t and (b) dependence of $M_{n,SEC}$ (filled symbols) and PDIs (empty symbols) of the polymers on C_{MMA} for the $FeBr_2$-mediated ATRP of MMA with different amounts of initially added $FeCl_3$. $[MMA]_0/[EBIB]_0/[FeBr_2]_0/[FeCl_3]_0/[NHPMI]_0$ = 150/1/1/0/2 (●), 150/1/1/0.2/2.4 (▲), and 150/1/1/0.6/3.2 (■), MMA/2-butanone= 1/2 v/v, reaction temperature: 90 °C.

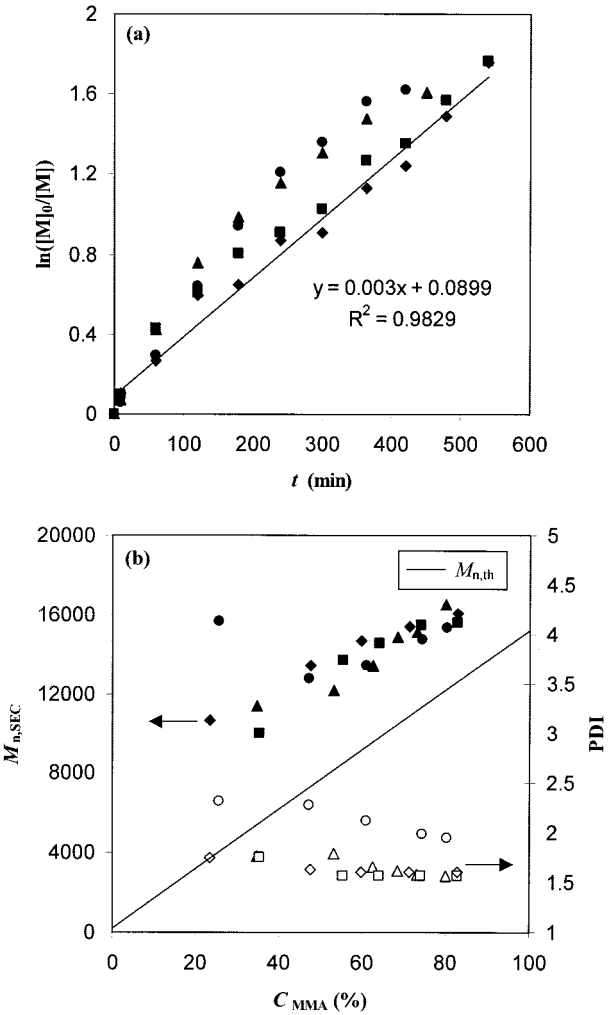

Figure 4. (a) Kinetic plots of $\ln([M]_0/[M])$ versus reaction time t and (b) dependence of $M_{n,SEC}$ (filled symbols) and PDIs (empty symbols) of the polymers on C_{MMA} for the $FeCl_2$-mediated ATRP of MMA with different amounts of initially added $FeCl_3$. $[MMA]_0/[EBIB]_0/[FeCl_2]_0/[FeCl_3]_0/[NHPMI]_0$ = 150/1/1/0/2 (●), 150/1/1/0.2/2.4 (▲), 150/1/1/0.4/2.8 (■), and 150/1/1/0.6/3.2 (◆), MMA/2-butanone= 1/2 v/v, reaction temperature: 90 °C.

polymerization. Compared with the curved kinetic plot of $\ln([M]_0/[M])$ versus t at 90 °C, a linear kinetic plot was obtained when the reaction was carried out at 75 °C [Fig. 5(a)], revealing that radical termination was minimized at a lower reaction temperature. The polymerization at 75 °C, however, provided polymers with slightly higher PDIs than those obtained at 90 °C [Fig. 5(b)], probably because of a higher k_p/k_t value and/or a faster exchange between the dormant specie (alkyl halide) and active specie (radical) in the ATRP system at higher temperatures.[52] Therefore, a reaction temperature of 90 °C was chosen in the following studies.

Effect of Molar Ratio of Iron Halide to NHPMI on Polymerization Behavior

The iron halide mediated ATRP of MMA with EBIB as the initiator was also carried out with a molar ratio of iron halide to NHPMI of 1 to study its effect on polymerization [Fig. 6(a,b)]. To improve the controllability of the system, 20% of iron(III) halide relative to iron(II) halide was added at the beginning of the reactions. The ki-

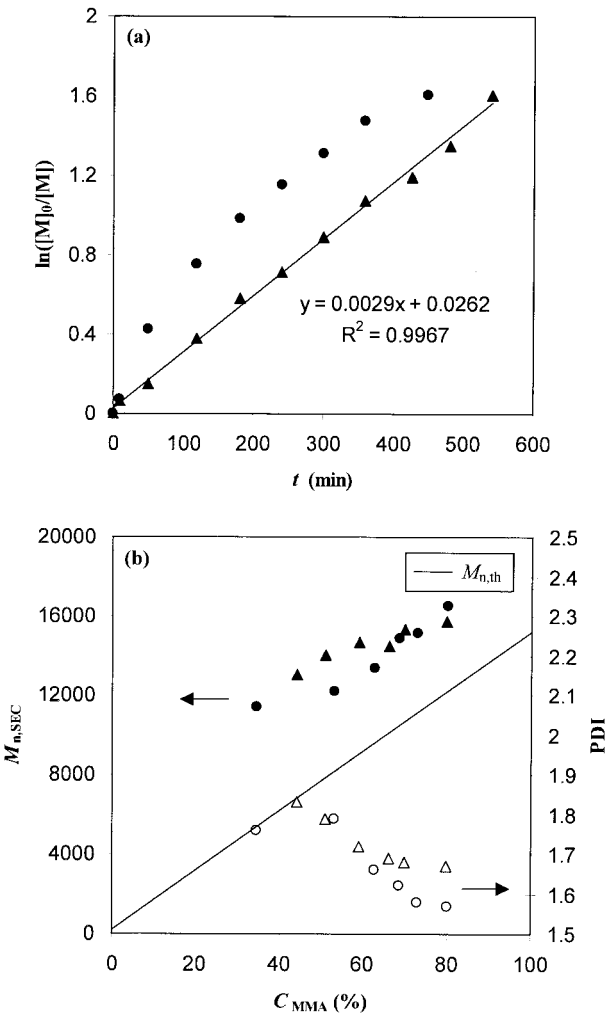

Figure 5. (a) Kinetic plots of $\ln([M]_0/[M])$ versus reaction time t and (b) dependence of $M_{n,SEC}$ (filled symbols) and PDIs (empty symbols) of the polymers on C_{MMA} for ATRP with $[MMA]_0/[EBIB]_0/[FeCl_2]_0/[FeCl_3]_0/[NHPMI]_0$ = 150/1/1/0.2/2.4 at 75 (▲) and 90 (●) °C, respectively. MMA/2-butanone = 1/2 v/v.

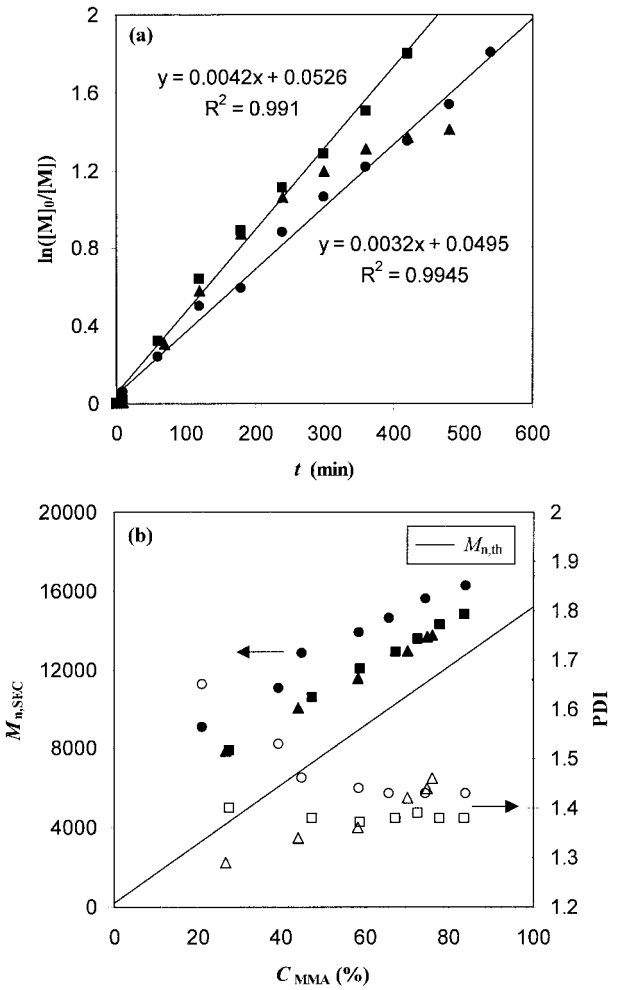

Figure 6. (a) Kinetic plots of $\ln([M]_0/[M])$ versus reaction time t and (b) dependence of $M_{n,SEC}$ (filled symbols) and PDIs (empty symbols) of the polymers on C_{MMA} for the ATRP of MMA with $[MMA]_0/[EBIB]_0/[FeX_2]_0/[FeY_3]_0/[NHPMI]_0$ = 150/1/1/0.2/1.2 [X = Y = Br (▲), X = Br, Y = Cl (■), and X = Y = Cl (●)], MMA/2-butanone = 1/2 v/v, reaction temperature: 90 °C.

netic plots of $\ln([M]_0/[M])$ versus t were linear for the ATRP with $[MMA]_0/[EBIB]_0/[FeX_2]_0/[FeCl_3]_0/[NHPMI]_0$ = 150/1/1/0.2/1.2 (X = Br and Cl) [Fig. 6(a)], whereas the ATRP of MMA with $[MMA]_0/[EBIB]_0/[FeX_2]_0/[FeCl_3]_0/[NHPMI]_0$ = 150/1/1/0.2/2.4 (X = Br and Cl) provided curved kinetic plots [Figs. 3(a) and 4(a)], indicating that the polymerization was better controlled in the former case. The $M_{n,SEC}$ of the polymers prepared via ATRP with [iron halide]$_0$/$[NHPMI]_0$ = 1 increased linearly with C_{MMA} throughout the reactions, and polymers with lower PDIs were obtained in this case, than those obtained from ATRP with [iron halide]$_0$/$[NHPMI]_0$ = 1/2 [see Figs. 3(b), 4(b), and 6(b)]. The ATRP of MMA with $[MMA]_0/[EBIB]_0/[FeBr_2]_0/[FeCl_3]_0/[NHPMI]_0$ = 150/1/1/0.2/1.2 provided the optimal results (PDI = 1.38 and initiation efficiency $f = M_{n,th}/M_{n,SEC}$ = 0.87 at a C_{MMA} = 84%) among all the studied systems. It is worth noting that the ATRP with $[MMA]_0/[EBIB]_0/[FeBr_2]_0/[FeBr_3]_0/[NHPMI]_0$ = 150/1/1/0.2/1.2 provided polymers with rather low PDIs at low C_{MMA} (PDI = 1.29 at a C_{MMA} = 27%). However, the PDIs of the polymers increased with C_{MMA} and reached 1.46 at a C_{MMA} = 76% [Fig. 6(b)]. This, together with the curved kinetic plot [Fig. 6 (a)], indicates the presence of radical termination during the reaction.

Iron Halide Mediated ATRP of MMA with TsCl as the Initiator

TsCl has proven to be a universal initiator for the ATRP of methacrylates, styrene derivatives, and acrylates, and TsCl-initiated ATRP of MMA usually shows high initiation efficiency and provides polymers with low PDIs, because of its specific initiation process.[53] Therefore, TsCl was also utilized in this study. The ATRP with $[MMA]_0/[TsCl]_0/[FeX_2]_0/[NHPMI]_0$ = 150/1/1/2 (X = Br and Cl) were conducted in dry 2-butanone at 90 °C with a volume ratio of 2-butanone to MMA of 2. The kinetic plots of $\ln([M]_0/[M])$ versus t were curved for the studied systems [Fig. 7(a), X = Br (▲) and Cl (◆)], revealing the occurrence of radical termination. The $M_{n,SEC}$ increased linearly with C_{MMA}, but were much higher than $M_{n,th}$ [Fig. 7(b)]. The PDIs of the polymers prepared via the $FeBr_2$-mediated ATRP increased from 1.55 to 1.86 with the increase of C_{MMA} from 26% to 70%. On the other hand, the $FeCl_2$-mediated ATRP was totally uncontrolled, where bimodal molecular weight distributions were observed for all the obtained polymers, and the PDIs of the polymers were larger than 2.3.

Effect of Initially Added Iron(III) Halide on the Polymerization Process

Iron(III) halide was also added into the TsCl-initiated ATRP of MMA with $([FeBr_2]_0+[FeX_3]_0)/[NHPMI]$ = 1/2 (X = Br and Cl) at the beginning of the reaction to improve the controllability of the polymerization. However, the initially added iron(III) halide showed a negative effect on the controllability of the polymerization, that is, the kinetic plots became more curved, the initiation efficiency, *f,* of the systems decreased, and PDIs of the polymers increased with the addition of iro-

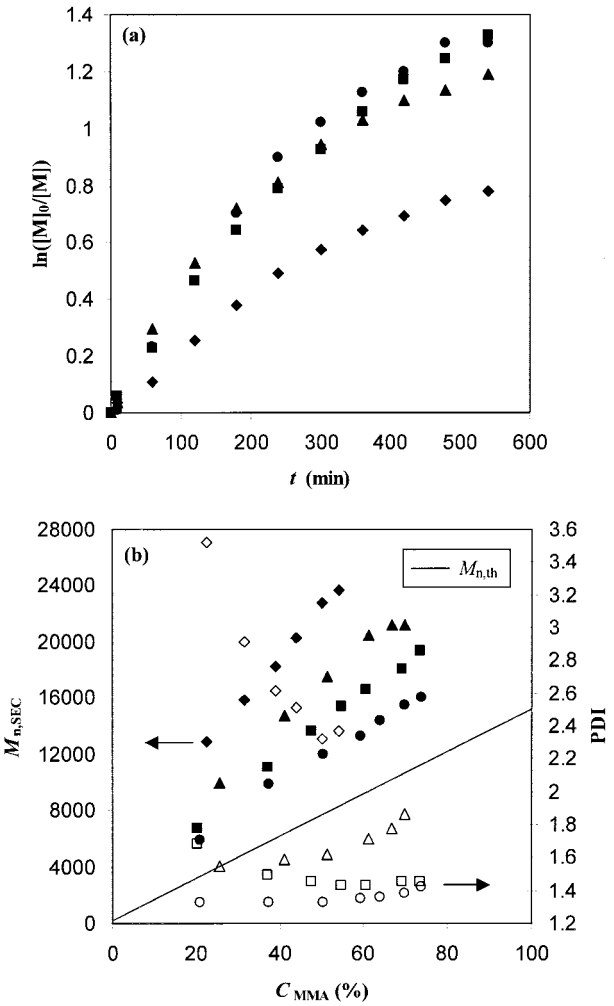

Figure 7. (a) Kinetic plots of $\ln([M]_0/[M])$ versus reaction time t and (b) dependence of $M_{n,SEC}$ (filled symbols) and PDIs (empty symbols) of the polymers on C_{MMA} for the TsCl-initiated ATRP of MMA. $[MMA]_0/[TsCl]_0/[FeX_2]_0/[NHPMI]_0$ = 150/1/1/2 [X = Br (▲) and Cl (◆)] and 150/1/1/1 [X = Br (●) and Cl (■)], MMA/2-butanone= 1/2 v/v, reaction temperature: 90 °C.

n(III) halide [Fig. 8(a,b)]. Further, the amount of the initially added iron(III) halide also had a great influence on the reactions. The more the initially added iron(III) halide, the worse the controllability of the reactions. These phenomena need further investigation.

Effect of Molar Ratio of Iron Halide to NHPMI on Polymerization Behavior

The TsCl-initiated ATRP of MMA with $[MMA]_0/[TsCl]_0/[FeX_2]_0/[NHPMI]_0$ = 150/1/1/1 were also carried out in order to compare with polymerization using $[MMA]_0/[TsCl]_0/[FeX_2]_0/[NHPMI]_0$ = 150/1/1/2 (X = Br and Cl) (Fig. 7). The polymerization rates of the $FeBr_2$-mediated ATRP were only slightly influenced by the molar ratio of $FeBr_2$ to NHPMI, whereas the $FeCl_2$-mediated ATRP with $[FeCl_2]_0/[NHPMI]_0$ = 1 proceeded much faster than that with $[FeCl_2]_0/[NHPMI]_0$ = 1/2 [Fig. 7(a)]. Similar to the EBIB-initiated ATRP system, the TsCl-initiated system also became better controlled in terms of PDIs of the obtained polymers and f of the reactions when $[FeX_2]_0/[NHPMI]_0$ = 1 [Fig. 7(b)]. Moreover, the $FeBr_2$-mediated ATRP proved to be better con-

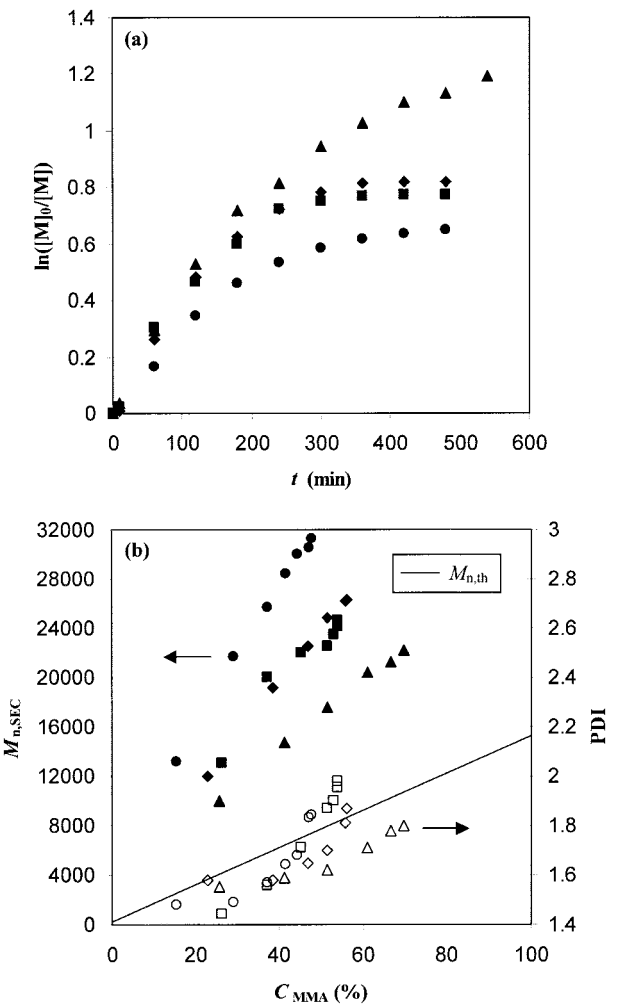

Figure 8. (a) Kinetic plots of $\ln([M]_0/[M])$ versus reaction time t and (b) dependence of $M_{n,SEC}$ (filled symbols) and PDIs (empty symbols) of the polymers on C_{MMA} for the TsCl-initiated ATRP of MMA with different amounts of initially added iron(III) halide. $[MMA]_0/[TsCl]_0/[FeBr_2]_0/[FeX_3]_0/[NHPMI]_0$ = 150/1/1/0/2 (▲), 150/1/1/0.2/2.4 [X = Cl(◆)], and 150/1/1/0.6/3.2 [X = Br (■) and Cl (●)], MMA/2-butanone = 1/2 v/v, reaction temperature: 90 °C.

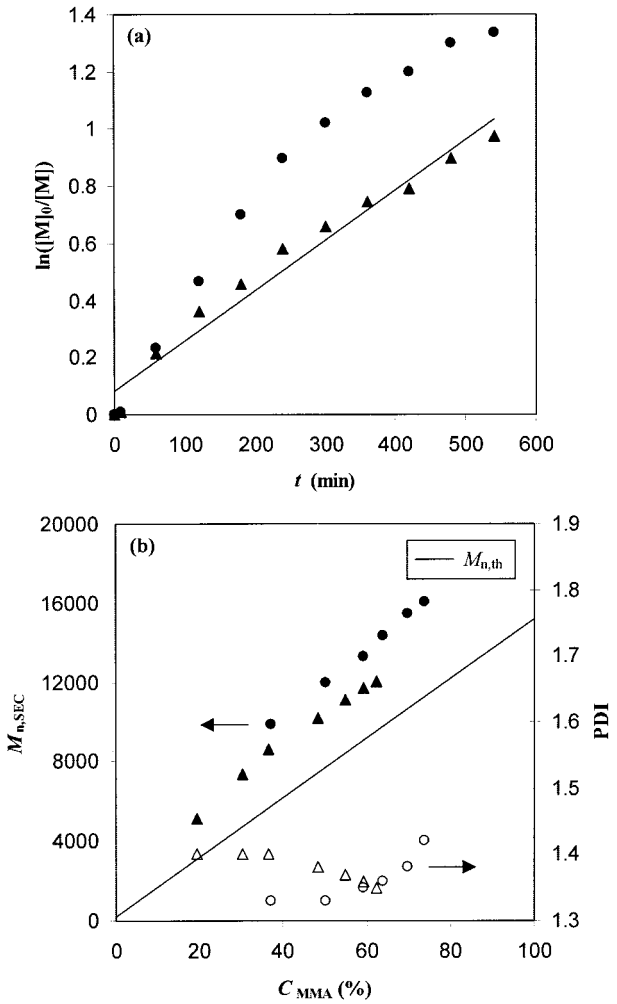

Figure 9. Effect of iron halide and NHPMI concentrations on the TsCl-initiated ATRP of MMA. $[MMA]_0/[TsCl]_0/[FeBr_2]_0/[NHPMI]_0$ = 150/1/1/1 (●) and 150/1/0.5/0.5 (▲), MMA/2-butanone = 1/2 v/v, reaction temperature: 90 °C.

trolled than the $FeCl_2$-mediated one, and higher f and polymers with lower PDIs were obtained in the former case. It is worth noting that the PDIs of the polymers obtained from the TsCl-initiated ATRP with $[FeBr_2]_0/[NHPMI]_0 = 1$ increased slightly with C_{MMA} [Figs. 7(b) and 9(b)], indicating the presence of radical termination during the polymerization.

Effect of Iron Halide and NHPMI Concentrations on the Polymerization Process

To minimize radical termination in the ATRP with $[MMA]_0/[TsCl]_0/[FeBr_2]_0/[NHPMI]_0$ = 150/1/1/1, the concentrations of $FeBr_2$ and NHPMI were reduced to half amounts.[47] As expected, the polymerization rate decreased with the decrease of $FeBr_2$ and NHPMI concentrations. Radical termination was minimized, as demonstrated by the linear kinetic plot [Fig. 9(a), symbol ▲]. The PDIs of the polymers decreased with C_{MMA} and reached 1.35 at a C_{MMA} = 62% [Fig. 9(b)]. Besides, the f value of the reaction also increased.

Influence of Purification Methods on Properties of the Obtained Polymers

In order to compare with the literature results,[42] some polymers were also purified by precipitation from 20-fold volume excess of rapidly stirred acidified methanol solutions (5% HCl, v/v) instead of simply passing through aluminum oxide columns before SEC measurements. Table 1 shows that purification methods indeed influenced the $M_{n,SEC}$ and PDIs of the obtained polymers and thus the f values of the reactions. Polymers purified by precipitation showed higher $M_{n,SEC}$ and lower PDIs than those purified by simply passing through aluminum oxide columns, suggesting that low-molecular-weight PMMAs were soluble in acidified methanol. This was further confirmed by the fact that the lower the molecular weights of the polymers, the larger the changes of the $M_{n,SEC}$ and PDIs of the polymers after precipitation (Table 1). Polymers with PDIs of approximately 1.25 were obtained for the studied systems at relatively high C_{MMA}, with the same purification procedure as that described in the literature, where polymers with PDIs = 1.49–1.64 were obtained, even in the optimal system [with 2-(*N*-cyclododecylimino)-6-methylpyridine as the ligand].[42]

End Group Analysis of a Polymer Prepared via ATRP

A PMMA sample with an $M_{n,SEC}$ = 10,060 and PDI = 1.18 was prepared via the ATRP with $[MMA]_0/[TsCl]_0/[FeBr_2]_0/[NHPMI]_0$ = 150/1/0.5/0.5 at 90 °C in 2 h [C_{MMA} = 32%, a repeated reaction for system 2 in Table 1; the polymer was purified by precipitating from a 20-fold volume excess of acidified methanol solution (5% HCl, v/v)]. Figure 10 shows the ^1H NMR spectrum of the polymer in CD_2Cl_2. The characteristic signals corresponding to the phenyl protons and methyl protons of the *p*-toluenesulfonyl group were observed around 7.2–7.9 and 2.45 ppm as multiple peaks and a single peak, respectively. The signals corresponding to the methylene protons in the MMA unit connected with the *p*-toluenesulfonyl group were observed around 3.10 ppm.[54] The sig-

Table 1. Results of Iron Halide Mediated ATRP of MMA with Different Purification Processes for Polymers

System[a]	t (min)[b]	C_{MMA} (%)	$M_{n,th}$	$M_{n,SEC}$[c]	PDI[c]	f[c,e]	$M_{n,SEC}$[d]	PDI[d]	f[d,e]
1	125	47	7,250	10580	1.38	0.69	13,340	1.21	0.54
1	180	59	9,060	12030	1.37	0.75	14,400	1.23	0.63
1	300	72	11,010	13550	1.39	0.81	15,430	1.27	0.71
1	420	84	12,810	14780	1.38	0.87	16,520	1.26	0.78
2	60	19	3,040	5130	1.40	0.59	7,920	1.17	0.38
2	120	30	4,700	7400	1.40	0.64	9,850	1.22	0.48
2	300	48	7,400	10210	1.38	0.72	12,340	1.24	0.60
2	420	55	8,450	11140	1.37	0.76	13,250	1.24	0.64
2	540	62	9,500	12010	1.35	0.79	13,960	1.24	0.68

[a] System 1: $[MMA]_0/[EBIB]_0/[FeBr_2]_0/[FeCl_3]_0/[NHPMI]_0$ = 150/1/1/0.2/1.2; System 2: $[MMA]_0/[TsCl]_0/[FeBr_2]_0/[NHPMI]_0$ = 150/1/0.5/0.5.
[b] Reaction time.
[c] The polymers were purified by passing through neutral aluminum oxide columns.
[d] The polymers were purified by precipitation from 20-fold volume excess of acidified methanol solutions (5% HCl, v/v).
[e] f refers to the initiation efficiency ($f = M_{n,th}/M_{n,SEC}$).

nal corresponding to the methyl protons of $COOCH_3$ in the MMA unit connected with the halide end group was observed at approximately 3.74 ppm.[55,56] In addition, some signals appeared between 2.40–2.90 ppm, which corresponded to the methylene protons in the MMA unit connected with the halide end group. These verified the presence of a halide end group in the polymer and the occurrence of the polymerization according to the described ATRP mechanism.[6,7] The polymer proved to be end-capped with both chlorine and bromine atoms, as demonstrated by the presence of signals around 2.50 and 2.72 ppm, respectively.[55,56] The integration ratio of the signals corresponding to the methyl protons of the *p*-toluenesulfonyl group and the methylene protons in the MMA unit connected with the halide end group (2.35–2.90 ppm), to those corresponding to the phenyl protons of the *p*-toluenesulfonyl group (7.2–7.9 ppm) was about 1.20, which agreed quite well with the theoretical value of 1.25. This showed that the functionality of the halide end group was close to unity. A number-average molecular weight of 10,680 was obtained for the polymer by comparing the integrations of signals corresponding to the phenyl protons of the *p*-toluenesulfonyl group and methyl protons of $COOCH_3$ in the MMA repeat unit in the polymer backbone and by assuming that one polymer chain contains one phenyl group, which was in good agreement with the value obtained from SEC ($M_{n,SEC}$ = 10060). In addition, the stereochemical structures (rr = 59%) of the polymer were similar with those prepared via the conventional radical polymerization (rr = 58–64%).[57,58]

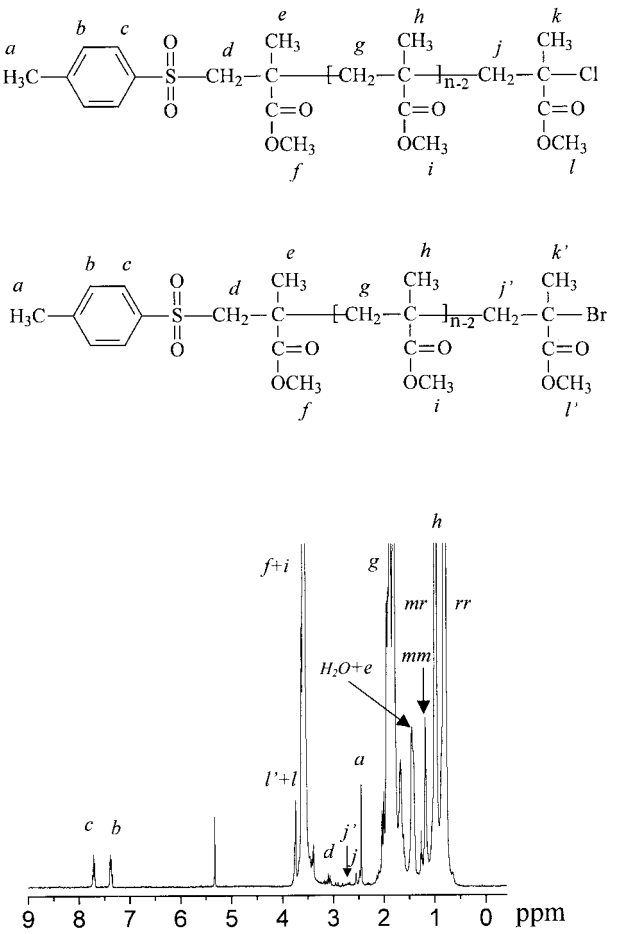

Figure 10. ^1H NMR spectrum (solvent: CD_2Cl_2) of a polymer ($M_{n,SEC}$ = 10060 and PDI = 1.18) prepared via the ATRP of MMA with $[MMA]_0/[TsCl]_0/[FeBr_2]_0/[NHPMI]_0$ = 150/1/0.5/0.5 at 90 °C in 2 h (mm: isotactic; mr: heterotactic; rr: syndiotactic).

An additional method for verifying the functionality of a polymer prepared via ATRP is its use as a macroinitiator for the same or other monomers. A chain-extension of the same PMMA sample with MMA was conducted at 90 °C in 2-butanone with $[MMA]_0/[macroinitiator]_0/[FeBr_2]_0/[FeCl_3]_0/[NHPMI]_0$ = 1500/0.4/3/0.6/3.6 and MMA/2-butanone = 1/2 v/v. A linear kinetic plot of $\ln([M]_0/[M])$ versus t was obtained [Fig. 11(a)], showing that radical termination was negligible during the chain-extension reaction. A chain-extended PMMA with an $M_{n,SEC}$ of 41130 and PDI of 1.38 and another one with an $M_{n,SEC}$ of 60070 and PDI of 1.57 were obtained after a reaction time of 2 and 4 h, respectively [Fig. 11(b)]. The chain-extended polymers were purified by precipitating from a 20-fold volume excess of acidified methanol solution (5% HCl, v/v). The large increase of the molecular weights and the unimodal shapes of the SEC traces of the chain-extended polymers demonstrated the success of the chain-extension. The absence of significant shoulders on the low-molecular-weight sides of the SEC traces of the chain-extended polymers again indicated that the chain end functionality of the macroinitiator was high. However, some tailing was observed for the SEC traces of the chain-extended polymers. Also, their PDIs were higher than that of the macroinitiator and increased slightly with C_{MMA}, which was likely caused by the slow initiation of the macroinitiator for the chain-extension reaction.

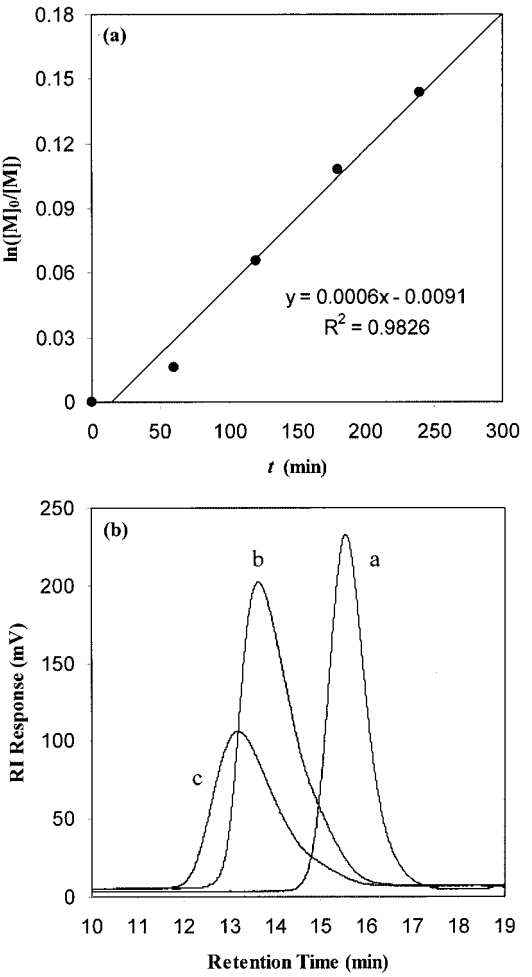

Figure 11. (a) Kinetic plot of $\ln([M]_0/[M])$ versus reaction time t for the chain-extension reaction at 90 °C in 2-butanone ($[MMA]_0/[macroinitiator]_0/[FeBr_2]_0/[FeCl_3]_0/[NHPMI]_0$ = 1500/0.4/3/0.6/3.6, MMA/2-butanone = 1/2 v/v) and (b) SEC traces of a macroinitiator ($M_{n,SEC}$ = 10060 and PDI = 1.18, line a) and its chain-extended polymers obtained at 2 h ($M_{n,SEC}$ = 41130 and PDI = 1.38, line b) and 4 h ($M_{n,SEC}$ = 60070 and PDI = 1.57, line c), respectively.

Cyclic Voltammetry (CV)

To obtain a better understanding of the differing catalytic behaviors of the *in situ*-formed complexes by iron halide and NHPMI with different molar ratios, their redox potentials and reversibility were analyzed by cyclic voltammetry (CV). A typical cyclic voltammogram for the *in situ*-formed complex by $FeBr_2$ and NHPMI with a molar ratio of 1 in dry 2-butanone is shown in Figure 12. The main feature at approximately 1.1 V was attributed to the reversible iron(II)/iron(III) couple relevant to ATRP catalysis, and a second feature at approximately −0.1 V was assigned to the iron(I)/iron(II) couple. All complexes 1–4 (see Table 2) were found to possess surprisingly high $E_{1/2}$ values (typically ca. 1100 mV), as reported previously.[42] The ΔE_p(complex) was 120 and 180 mV for complex 1 and 2, respectively (Table 2, $E_{1/2}$ = 450 mV and ΔE_p = 280 mV for ferrocene), which appeared to correlate well with their catalytic activity.[39,42] However, there was little difference between the ΔE_p(complex) values of complexes 3 and 4. The larger steric hindrance of complex 4 to the halogen transfer in ATRP than complex 3, because of the different numbers of coordinating ligand available, might be responsible for their differing catalytic behavior. Further, this steric hindrance effect might also be the reason for the large differences between the polymerization rates of the TsCl-initiated ATRP catalyzed by complexes 3 and 4 [Fig. 7(a)].

CONCLUSIONS

This article describes systematic studies on the iron halide mediated ATRP of MMA with NHPMI as the ligand and EBIB/TsCl as the initiator, where fast polymerizations, linear progress of molecular weights with monomer conversions, and low polydispersities of the polymers were achieved under optimal reaction conditions. 2-Butanone proved to be a better solvent than *p*-xylene, in terms of polymerization rate and molecular weight control for the EBIB-initiated ATRP, and was subsequently used in all the studied systems. The addition of iron(III) halide into the EBIB-initiated ATRP system with $[\text{iron halide}]_0/[\text{NHPMI}]_0 = 1/2$ at the beginning of the reactions improved the controllability of the polymerization. The $M_{n,SEC}$ started to increase with C_{MMA} and PDIs of the polymers decreased greatly with the initially added iron(III) halide relative to iron(II) halide $\geq$ 20%, although they were still rather high (PDIs $\geq$ 1.57). The decrease of the reaction temperature from 90 to 75 °C led to less radical termination, but the PDIs of the polymers slightly increased, probably because of the unfavorable effect on the k_p/k_t value and/or the exchange rate between the dormant specie (alkyl halide) and active specie (radical) in the ATRP system. In contrast to the EBIB-initiated ATRP system, the controllability of the TsCl-initiated system decreased with the addition of iron(III) halide at the beginning of reactions. The molar ratio of iron halide to NHPMI had a significant impact on the controllability of both EBIB and TsCl-initiated ATRP systems. The ATRP systems with $[\text{iron halide}]_0/[\text{NHPMI}]_0 = 1/2$ provided polymers with PDIs $\geq$ 1.57, whereas those with $[\text{iron halide}]_0/[\text{NHPMI}]_0 = 1$ resulted in polymers with PDIs as low as 1.35 at relatively high C_{MMA}. Furthermore, polymers with PDIs around 1.25 were obtained for the studied systems at relatively high C_{MMA} after they were purified by precipitation from acidified methanol. ^{1}H NMR characterization and chain-extension reaction of a polymer prepared via ATRP showed the presence of halide end groups and their high functionality. In addition, CV measurements showed that the differing catalytic behaviors of the *in situ*-formed complexes by $FeBr_2$ and NHPMI with different molar ratios could be mainly ascribed to their differing ΔE_p values, whereas the steric hindrance effect might be responsible for the differing catalytic behavior of the complexes formed by $FeCl_2$ and NHPMI with different molar ratios. In future high throughput experimentation methods will be utilized for subsequent studies.

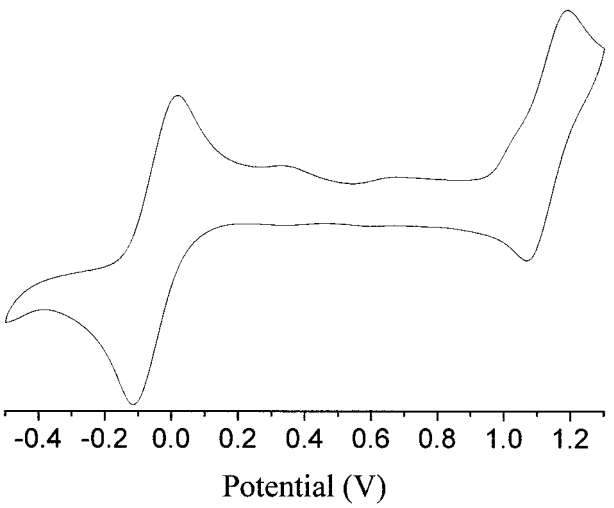

Figure 12. The cyclic voltammogram of the *in situ*-formed complex by $FeBr_2$ and NHPMI with a molar ratio of 1 in dry 2-butanone. Start potential: −500 mV, end potential: 1300 mV, sweep rate: 200 mV s^{-1}.

Table 2. Redox Potentials ($E_{1/2}$) and Peak Separations (ΔE_p) for Complexes[a]

Complex	$[FeX_2]_0/[\text{NHPMI}]_0$	X	$E_{1/2}$/mV	ΔE_p/mV
1	1:1	Br	1130	120
2	1:2	Br	1100	180
3	1:1	Cl	1120	110
4	1:2	Cl	1100	120

[a] $E_{1/2}$ = 450 mV and ΔE_p = 280 mV for ferrocene(II)/(III) couple in dry 2-butanone.

This work was financially supported by the Dutch Polymer Institute. The authors thank Wieb Kingma and Edwen Beckers for carrying out size exclusion chromatography (SEC) and cyclic voltammetry (CV) measurements, respectively.

REFERENCES AND NOTES

1. Controlled Radical Polymerization; Matyjaszewski, K., Ed.; ACS Symposium Series 685; American Chemical Society: Washington, DC, 1998.
2. Controlled/Living Radical Polymerization—Progress in ATRP, NMP, and RAFT, Matyjaszewski, K., Ed.; ACS Symposium Series 768; American Chemical Society: Washington, DC, 2000.
3. Controlled/Living Radical Polymerization; Matyjaszewski, K., Ed.; ACS Symposium Series 854; American Chemical Society: Washington, DC, 2003.

4. Matyjaszewski, K.; Xia, J. Chem Rev 2001, 101, 2921.
5. Kamigaito, M.; Ando, T.; Sawamoto, M. Chem Rev 2001, 101, 3689.
6. Wang, J. S.; Matyjaszewski, K. J Am Chem Soc 1995, 117, 5614.
7. Wang, J. S.; Matyjaszewski, K. Macromolecules 1995, 28, 7901.
8. Percec, V.; Barboiu, B. Macromolecules 1995, 28, 7970.
9. Patten, T. E.; Xia, J.; Abernathy, T.; Matyjaszewski, K. Science 1996, 272, 866.
10. Matyjaszewski, K.; Patten, T. E.; Xia, J. J Am Chem Soc 1997, 119, 674.
11. Percec, V.; Asandei, A. D.; Asgarzadeh, F.; Bera, T. K.; Barboiu, B. J Polym Sci Part A: Polym Chem 2000, 38, 3839.
12. Nanda, A. K.; Matyjaszewski, K. Macromolecules 2003, 36, 1487.
13. Kato, M.; Kamigaito, M.; Sawamoto, M.; Higashimura, T. Macromolecules 1995, 28, 1721.
14. Simal, F.; Demonceau, A.; Noels, A. F. Angew Chem Int Ed 1999, 38, 538.
15. Kamigaito, M.; Watanabe, Y.; Ando, T.; Sawamoto, M. J Am Chem Soc 2002, 124, 9994.
16. Hamasaki, S.; Kamigaito, M.; Sawamoto, M. Macromolecules 2002, 35, 2934.
17. Opstal, T.; Verpoort, F. Angew Chem Int Ed 2003, 42, 2876.
18. Lecomte, P.; Drapier, I.; Dubois, P.; Teyssié, P.; Jérôme, R. Macromolecules 1997, 30, 7631.
19. Moineau, G.; Granel, C.; Dubois, P.; Jérôme, R.; Teyssié, P. Macromolecules 1998, 31, 542.
20. Granel, C.; Dubois, P.; Jérôme, R.; Teyssié, P. Macromolecules 1996, 29, 8576.
21. Uegaki, H.; Kotani, Y.; Kamigaito, M.; Sawamoto, M. Macromolecules 1997, 30, 2249.
22. Uegaki, H.; Kotani, Y.; Kamigaito, M.; Sawamoto, M. Macromolecules 1998, 31, 6756.
23. Moineau, G.; Minet, M.; Dubois, P.; Senninger, T.; Teyssié, P.; Jérôme, R. Macromolecules 1999, 32, 27.
24. Kotani, Y.; Kamigaito, M.; Sawamoto, M. Macromolecules 1999, 32, 2420.
25. Grognec, E. L.; Claverie, J.; Poli, R. J Am Chem Soc 2001, 123, 9513.
26. Stoffelbach, F.; Poli, R.; Richard, P. J Organomet Chem 2002, 663, 269.
27. Wang, B.; Zhuang, Y.; Luo, X.; Xu, S.; Zhou, X. Macromolecules 2003, 36, 9684.
28. Ando, T.; Kamigaito, M.; Sawamoto, M. Macromolecules 1997, 30, 4507.
29. Matyjaszewski, K.; Wei, M.; Xia, J.; McDermott, N. E. Macromolecules 1997, 30, 8161.
30. Takahashi, H.; Ando, T.; Kamigaito, M.; Sawamoto, M. Macromolecules 1999, 32, 3820.
31. Kotani, Y.; Kamigaito, M.; Sawamoto, M. Macromolecules 1999, 32, 6877.
32. Teodrescu, M.; Gaynor, S. G.; Matyjaszewski, K. Macromolecules 2000, 33, 2335.
33. Louis, J.; Grubbs, R. H. Chem Commun 2000, 1479.
34. Kotani, Y.; Kamigaito, M.; Sawamoto, M. Macromolecules 2000, 33, 3543.
35. Göbelt, B.; Matyjaszewski, K. Macromol Chem Phys 2000, 201, 1619.
36. Zhu, S.; Yan, D. Macromolecules 2000, 33, 8233.
37. Wakioka, M.; Beak, K. Y.; Ando, T.; Kamigaito, M.; Sawamoto, M. Macromolecules 2002, 35, 330.
38. Detrembleur, C.; Teyssié, P.; Jérôme, R. Macromolecules 2002, 35, 1611.
39. Gibson, V. C.; O'Reilly, R. K.; Reed, W.; Wass, D. F.; White, A. J. P.; Williams, D. J. Chem Commun 2002, 1850.
40. Gibson, V. C.; O'Reilly, R. K.; Wass, D. F.; White, A. J. P.; Williams, D. J. Macromolecules 2003, 36, 2591.
41. O'Reilly, R. K.; Gibson, V. C.; White, A. J. P.; Williams, D. J. J Am Chem Soc 2003, 125, 8450.
42. Gibson, V. C.; O'Reilly, R. K.; Wass, D. F.; White, A. J. P.; Williams, D. J. J Chem Soc Dalton Trans 2003, 2824.
43. Haddleton, D. M.; Jasieczek, C. B.; Hannon, M. J.; Shooter, A. J. Macromolecules 1997, 30, 2190.
44. Haddleton, D. M.; Kukulj, D.; Duncalf, D. J.; Heming, A. M.; Shooter, A. J. Macromolecules 1998, 31, 5201.
45. Haddleton, D. M.; Crossman, M. C.; Dana, B. H.; Duncalf, D. J.; Heming, A. M.; Kukulj, D.; Shooter, A. J. Macromolecules 1999, 32, 2110.
46. Zhang, H.; Klumperman, B.; Ming, W.; Fischer, H.; van der Linde, R. Macromolecules 2001, 34, 6169.
47. Zhang, H.; Klumperman, B.; van der Linde, R. Macromolecules 2002, 35, 2261.
48. Amass, A. J.; Wyres, C. A.; Colclough, E.; Marcia Hohn, I. Polymer 2000, 41, 1697.
49. Perrier, S.; Berthier, D.; Willoughby, I.; BattCoutrot, D.; Haddleton, D. M. Macromolecules 2002, 35, 2941.
50. Zhang, H.; van der Linde, R. J Polym Sci Part A: Polym Chem 2002, 40, 3549.
51. Zhang, H.; Schubert, U. S. Chem Commun 2004, 858.
52. Cheng, G. L.; Hu, C. P.; Ying, S. K. Macromol Rapid Commun 1999, 20, 303.
53. Percec, V.; Barboiu, B.; Kim, H. J. J Am Chem Soc 1998, 120, 305.
54. Percec, V.; Asandei, A. D.; Asgarzadeh, F.; Barboiu, B.; Holerca, M. N.; Grigoras, C. J Polym Sci Part A: Polym Chem 2000, 38, 4353.
55. Ando, T.; Kamigaito, M.; Sawamoto, M. Tetrahedron 1997, 53, 15445.
56. Zhang, H.; Jiang, X.; van der Linde, R. Polymer 2004, 45, 1455.
57. Feiring, A. E.; Wonchoba, E. R.; Davidson, F.; Percec, V.; Barboiu, B. J Polym Sci Part A: Polym Chem 2000, 38, 3313.
58. Yutaka, I.; Tamaki, N.; Yoshio, O. J Polym Sci Part A: Polym Chem 2001, 39, 1463.